A&A manuscript no.
(will be inserted by hand later)

Your thesaurus codes are:
11(11.19.2; 11.04.1; 12.12.1)

ASTRONOMY
AND
ASTROPHYSICS
1.2.2008

arXiv:astro-ph/9801197v2 2 Feb 1998

Research Note

The radial space distribution of KLUN-galaxies up to 200 Mpc: incompleteness or evidence for the behaviour predicted by fractal dimension ≈ 2?

P. Teerikorpi[1], **M. Hanski**[1], **G. Theureau**[2], **Yu. Baryshev**[3], **G. Paturel**[4], **L. Bottinelli**[2,5], **L. Gouguenheim**[2,5]

[1] Tuorla Observatory, FIN-21500 Piikkiö, Finland
[2] Observatoire de Paris-Meudon, CNRS URA1757, F-92195 Meudon Principal Cedex, France
[3] Astronomical Institute of the Saint-Petersburg University, 198904 St. Petersburg, Russia
[4] Observatoire de Lyon, F-69230 Saint-Genis Laval, France
[5] Université Paris-Sud, F-91405 Orsay, France

Received ; accepted

Abstract. We have studied using the KLUN sample of 5171 spiral galaxies having Tully-Fisher distance moduli, the average radial space distribution of galaxies out to a distance of about 200 Mpc (for $H_0 = 50$ km s^{-1} Mpc^{-1}). One motivation came from the debate on the fractal dimension $\mathcal{D}$ and maximum fractality scale $\lambda_{\rm max}$ of the large-scale galaxy distribution (Davis 1997, Guzzo 1997, Pietronero et al. 1997). A specific recent study is the 3-dimensional correlation analysis of the all-sky LEDA data base by Di Nella et al. (1996) who concluded that the galaxy distribution is fractal up to scales of at least 300 Mpc, with fractal dimension ≈ 2.2. One would expect to see a signal of this result in the radial space distribution of the all-sky KLUN sample. We have studied this question with a new method based on photometric TF distances, independent of redshift, to construct the number density distribution.

Our main results are:

1. While scattered below about 20 Mpc, at larger distances the radial distribution starts to follow, in terms of distance modulus $\mu_{\rm TF}$, the law $\log N = (0.46 \pm 0.01)\mu$+const., using diameter TF relation, and $\log N = (0.40 \pm 0.01)\mu$+const. for magnitudes. These are the predictions based on fractal dimensions 2.3 and 2.0, respectively. These radial density gradients are valid up to the limits of KLUN, or about 200 Mpc.
2. We have tried to understand the derived radial density behaviour as a result of some bias in KLUN or our analysis, however, without success. Numerical simulations have shown that the method itself works, though it somewhat underestimates the radial distribution exponent. If the density law is caused by incompleteness in the diameter limited KLUN sample, then the incompleteness should start at widely different angular diameters d_{25} for different values of rotation parameter $\log V_{\rm M}$, which would be quite unexpected. On the other hand, if the derived distribution is correct, the completeness is good down to $d_{25} = 1'.6$, as originally intended and previously concluded.
3. If correlation studies favoring long scale fractality (200 Mpc or more) and $\mathcal{D} \approx 2$ are correct, the position of our Galaxy would be close to average in the Universe, with the galaxy density decreasing around us according to the expected law (Mandelbrot 1982).

Key words: Galaxies: spiral – Galaxies: distances and redshifts – Cosmology: large-scale structure of Universe

1. Introduction

The present work is motivated by the longstanding problem in observational cosmology, concerning the structure of galaxy distribution: is the Universe homogeneous or fractal on large scales, and what is the scale where homogeneity begins? Paturel et al. (1994) and Witasse &

Send offprint requests to:

Paturel (1997) left open the possibility that the apparent partial incompleteness in some galaxy samples could actually reflect inhomogeneity or fractal distribution.

The completeness of the KLUN-sample of spiral galaxies was studied by Paturel et al. (1994) from the distribution of the angular sizes ($\log d_{25}$, with isophotal 25 mag/arcsec^2 diameters d_{25} expressed in units of $0'.1$). Separating the sample into parts with and without the plane of the Local Supercluster, it was concluded (on the assumption of homogeneity outside of the LS) that the sample is almost complete down to $\log d_{25} = 1.2$ (or $d_{25} = 1'.6$). In fact, it is a general problem, how to determine the completeness of a sample, if there is no a priori quarantee that the galaxy counts in a complete sample should follow, say, the distribution predicted by a homogeneous distribution of galaxies.

We continue here the study of incompleteness (the knowledge of which is crucial for our applications of KLUN), and attempt simultaneously to determine the all-sky average radial distribution of galaxies. This is done by a method which utilizes the TF distance moduli available for every KLUN galaxy. As the question of the radial distribution is closely connected with the problem of the scale and dimension of fractal distribution, we give below a short resumé of the state of this field.

The early history of determination of the fractal dimension and the maximum scale of fractality is described by Peebles (1980): the main result was that $\mathcal{D} \approx 1.2$ and $\lambda_{max} \leq 20$ Mpc[1]. The first evidence for a universal fractal distribution of galaxies with fractal dimension $\mathcal{D} \approx 2$ was given by Baryshev (1981) from number counts and virial mass distribution arguments. The same $\mathcal{D} \approx 2$ inside the Virgo supercluster was indicated by Klypin et al. (1989) from analysis of fractal properties of superclusters, with $\lambda_{max} < 40$ Mpc. Later in several works a double power law behaviour was found so that at distances $r \leq 6$ Mpc $\mathcal{D} \approx 1.2$, but for 6 Mpc $< r <$ 60 Mpc there is $\mathcal{D} \approx$ 2.2 (Einasto 1991, Guzzo et al. 1991, Calzetti et al. 1992, Einasto 1992, Guzzo 1997).

In recent years several extensive galaxy redshift surveys have become available (CfA1, CfA2, SSRS1, SSRS2, Perseus-Pisces, LEDA, LCRS, IRAS, etc., see the review by Sylos Labini et al. 1998a). Detailed analyses of the surveys have been made by different quantitative statistical methods which have revealed the fractal structure of the 3-dimensional galaxy distribution at the scales corresponding to the surveys. The fractality implies that around any galaxy the number density behaves with radius r as $n(r) = kr^{(\mathcal{D}-3)}$ for $r \leq \lambda_{max}$.

However, considerable debate has arisen on the value of fractal dimension $\mathcal{D}$ and the maximum correlation length λ_{max} (see e.g. Guzzo 1997, Sylos Labini et al. 1998b). One may even speak about two schools. According to the first one (see Davis 1997), using the standard correlation function analysis, fractal structure exists within the scale interval 0.02 Mpc $< r <$ 20 Mpc with dimension $\mathcal{D} \approx 1.2$, while on the scales larger than 40 Mpc the Universe becomes homogeneous. According to the second school (see Pietronero et al. 1997, Sylos Labini et al. 1998a), using a more general statistical approach which includes the correlation function method as a particular case, the fractal structure exists at least up to 200 Mpc and has dimension $\mathcal{D} \approx 2$. The debate shows the need for complementary approaches using other data and methods.

Recently, Di Nella et al. (1996) analyzed the correlation properties of the galaxy space distribution using the LEDA all-sky data base containing over 36000 galaxies with known redshifts. They concluded that the distribution has a fractal character up to the scales of 300 Mpc with the fractal dimension $\mathcal{D} \approx 2.2$. In a recent discussion, Guzzo (1997) concluded that the galaxies are clustered in a fractal way on small and intermediate scales, and the turnover to homogeneity may occur somewhere between 200 and 400 Mpc. Taken at face value, such results predict that in an all-sky sample like KLUN, one should see a radial galaxy number density behaviour which deviates from the uniform distribution. In terms of the distance modulus μ, uniformity corresponds to the differential law $\log N = 0.6\mu +$ constant for the number N of galaxies in the distance modulus range $\mu \pm 1/2\mu$, when μ has been derived by the "standard candle" method. In a distribution with fractal dimension $\mathcal{D}$, the expected density law around any galaxy is $\log N = 0.2\mathcal{D}\mu +$ constant, or with $\mathcal{D} = 2$, we have the "0.4μ-law".

There are a few noteworthy aspects in the present study. We concentrate on investigating how the radial density behaves around us, while the analyses mentioned above are usually based on the average behaviour around the different galaxies in the sample, which reveals the actual fractal law. However, there is special importance in seeing directly the behaviour around our individual vantage point. One thing is that we are naturally eager to see and check in concrete manner the "strange" prediction of fractality, or the thinning of average density, if our Galaxy occupies an average position in the fractal structure. On the other hand, Sylos Labini et al. (1996) have pointed out that in order to see the fractal behaviour around one point, one needs an all-sky sample with a sufficiently faint magnitude limit ($m \geq 14$) in order to avoid so-called finite-volume effect inside a few Voronoi-lengths. The KLUN sample can thus be used as a kind of first firm step for deriving the radial density law, which may be later straightforwardly extended deeper when the sample is gradually increased.

In order to derive the density law, we use a new method based on photometric (TF) distances. It has two special advantages. First, we can use almost the whole sample for constructing the density law. Second, unlike the methods based on redshift distances, we do not require a local veloc-

[1] All distances in this paper are based on $H_0 =$ 50 km s^{-1} Mpc^{-1}.

ity field model. In view of the recent suggestion (Praton et al. 1997) that working in the redshift space may enhance or even produce structures of the "Great Wall" type (and hence influence the correlation studies and presumably, the derived value of $\mathcal{D}$), it is especially important to use photometric distances in complementary studies.

2. The sample and the method

2.1. KLUN

The KLUN galaxy sample and the quality of the measured quantities of its members have been recently described by Theureau et al. (1997b). Originally intended to be complete down to the isophotal diameter $1'.6$, it now consists of 5171 galaxies covering the type range Sa – Sdm, having redshifts and the measured 21cm-line widths for the Tully-Fisher relation. 4577 galaxies have also the $B_{\rm T}$ magnitude.

For calculation of distance moduli μ, we use the direct TF relations established by Theureau et al. (1997b) and the same corrections for type effect, internal extinction, and galactic absorption. For example, the diameter TF relation gives the distance modulus μ as

$$\mu = 5(\log D_{25} - \log d_{25}^0 + \text{const.}),$$

where $\log D_{25} = a \log V_{\rm M} + b(T)$. In this formula, d_{25}^0 is the angular diameter corrected for galactic absorption and internal extinction, V_M is the maximum rotational velocity measured from the 21cm-line width of the galaxy, $b(T)$ is the TF zero point for galaxy type T, and a is the slope of the TF relation.

2.2. The method of TF distance moduli

We apply here a method outlined in Sect. 3 of Teerikorpi (1993), where the TF distance moduli can be used, in principle, up to the limits of the sample, in order to derive the form of the density law. The method utilizes galaxies in narrow $\log V_{\rm M}$ ranges to construct several differential distributions of μ, one for each $\log V_{\rm M}$ range. These distributions are displaced relative to each other in μ, because of different $\log V_{\rm M}$ (absolute magnitude) and the common diameter limit (or more exactly, the common incompleteness law). They have also generally different amplitudes, because different $\log V_{\rm M}$ ranges are populated by different numbers of galaxies, though their forms are similar if inside the ranges the galaxies are evenly distributed.

One expects that above some $\log d_{25}$, the sample is complete, hence below certain limits $\mu_{\rm lim}(\langle \log V_{\rm M} \rangle)$ each distribution reflects the true average space distribution. We illustrate this with Fig. 1 (see also Fig. 1 of Teerikorpi 1993), which helps one to understand why division of the sample into $\log V_{\rm M}$-ranges allows one *to separate the effect of true space density distribution from the effect of incompleteness in the distribution of* μ. After having identified this μ-range for the subsample with smallest $\langle \log V_{\rm M} \rangle$, hence smallest $\mu_{\rm lim}$, one can normalize the other subsamples to this one, shifting their $\log N$ vs. μ distributions vertically, so that up to $\mu_{\rm lim}$ all have the same average normalized number counts. This is allowed because for the subsamples with larger $\langle \log V_{\rm M} \rangle$, the complete μ-ranges extend beyond the $\mu_{\rm lim}$ corresponding to smaller $\langle \log V_{\rm M} \rangle$.

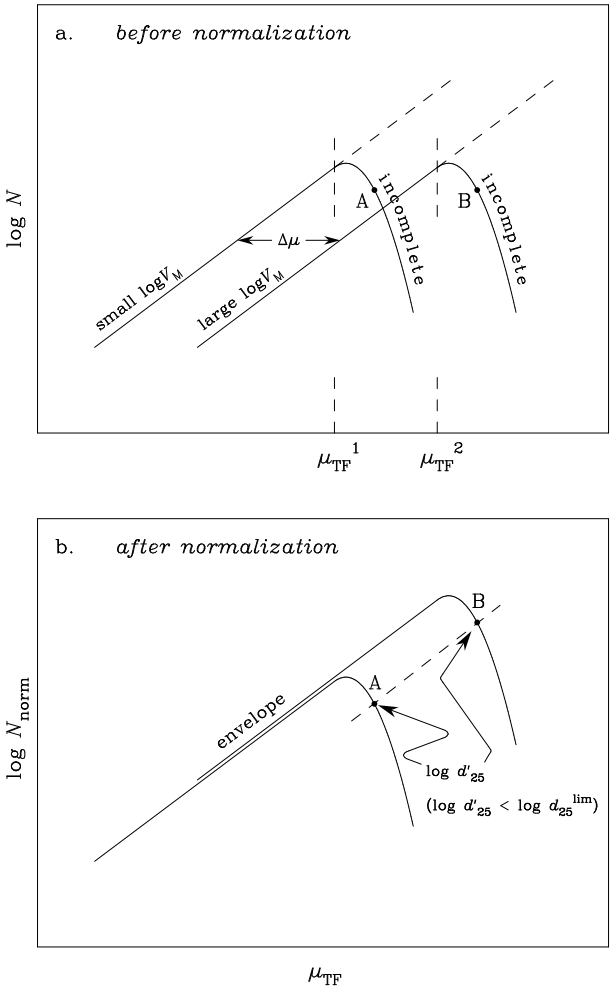

Fig. 1. Schematic illustration of how the distribution of TF distance moduli $\mu_{\rm TF}$ differ for two narrow $\log V_{\rm M}$ ranges separated from each other by $\Delta \log V_{\rm M}$. Here it is assumed that the true space distribution produces a constant slope in the $\log N$ vs. $\mu_{\rm TF}$ diagram (corresponding to density law $\rho(r) \propto r^{-\alpha}$). Small-$\log V_{\rm M}$ subsample reveals the correct density law up to $\mu_{\rm TF}^1$ where the incompleteness starting at $\log d_{25}^{\rm lim}$ begins to affect. Large-$\log V_{\rm M}$ subsample shows the same behaviour, though shifted towards larger $\mu_{\rm TF}$ by $\Delta\mu = 5a\Delta \log V_{\rm M}$. In the present method such distributions are in addition shifted vertically so that the complete parts come together forming a common envelope which follows the true space distribution law. Points A and B correspond to the same angular size d'_{25} in the incomplete region. After normalization they also define the correct density gradient.

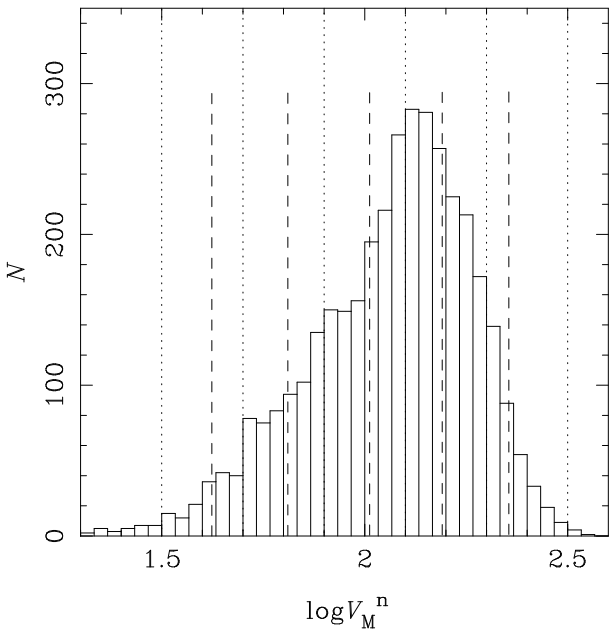

Fig. 2. $\log {V_{\rm M}}^{\rm n}$ distribution of the KLUN sample. Bins are separated with dotted lines. The dashed lines show the average values in each bin.

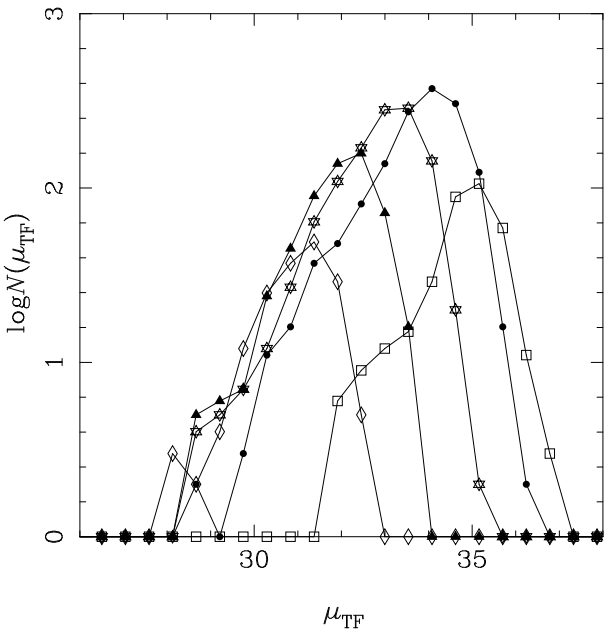

Fig. 3. Differential $\log N$ vs. $\mu_{\rm TF}$ (diameter) distributions for different $\log {V_{\rm M}}^{\rm n}$ ranges (see the text).

The common envelope of thus normalized distributions should follow the space distribution law up to the $\mu_{\rm lim}$ for the subsample with the largest $\langle \log V_{\rm M} \rangle$. An interesting feature of the method is that one may construct the space distribution still farther, as is shown by Fig. 1b where the points A and B corresponding to the same value of $\log d'_{25}$ ($< \log d_{25}^{\rm lim}$) in the incomplete region are connected by the line having the correct space density slope. The method is also quite simple in essence and allows one quickly to "see" the run of the density law and the factors influencing its derivation. Of course, working with real data is more problematic than the ideal theoretical case. For instance, one cannot use indefinitely small $\log V_{\rm M}$ ranges.

2.3. Special aspects

Actually, one must use the normalized $\log V_{\rm M}$ when making the described division of the sample:

$$\log {V_{\rm M}}^{\rm n} = \log V_{\rm M} - (\log d_{25}^{0} - \log d_{25})/a + (b(T) - b(6))/a$$

The concept of normalization has been introduced and discussed in a whole series of studies connected with the so-called method of normalized distances (see e.g. Theureau et al. 1997b). In this manner, galaxies of different types and with different inclination and galactic absorption corrections, but with equal normalized $\log {V_{\rm M}}^{\rm n}$, have the same effective limiting diameters. The $\mu_{\rm TF}$-distributions become thus better defined, and more closely follow the ideal distribution determined by the space density and incompleteness curves. In other words, for a given $\log {V_{\rm M}}^{\rm n}$, the $\mu_{\rm TF}$ scale reflects faithfully the $\log d_{25}$ scale.

Finally, we note that the method is in principle insensitive to the "patchy incompleteness" (Guzzo 1997) that may be present in such somewhat non-uniform collections of data as LEDA (the host database of KLUN which, however, was intended to be a homogeneous part of LEDA): In different regions of the sky the limiting diameters (magnitudes) may be different. Let us consider two regions, 1 and 2, where incompleteness starts at $\log d_{25}^{1}$ and $\log d_{25}^{2}$, respectively, and suppose we cannot identify these regions from the data. The summed relation, $\log (N_1 + N_2)$ vs. μ, for a constant $\log V_{\rm M}$ still follows the correct slope at small distances ($N_1 + N_2 = N_1 + c \cdot N_1 = (1 + c)N_1$, where the constant c depends only on the ratios of limiting angular sizes and region areas) while now the incomplete part of the curve is deformed. However, for different $\log V_{\rm M}$ the form of the curve is similar and the situation is analogous to what is depicted by Fig. 1.

3. Search for the density law

3.1. Diameter TF distance moduli

We show the procedure in a transparent manner which allows one to see the steps taken and to recognize the impact of possible systematic errors.

First, we have divided the sample into five $\log V_{\rm M}$ ranges according to the normalized $\log {V_{\rm M}}^{\rm n}$: 1.5 – 1.7 – 1.9 – 2.1 – 2.3 – 2.5. These intervals cover practically all the sample and the middle one is centered on the maximum of the $\log V_{\rm M}$ distribution (Fig. 2). Inside the extreme ranges the distributions are not symmetric around the mean, due to the systematic effect described in Sect. 3.3.

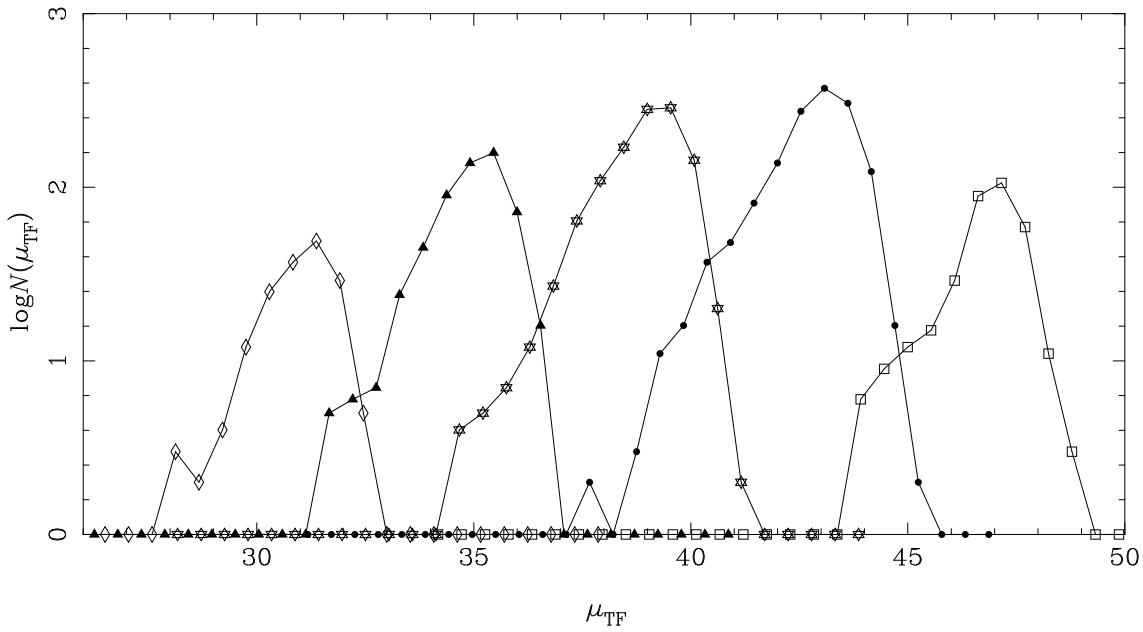

Fig. 4. As in Fig. 3, but now the distributions are arbitrarily shifted on the $\mu_{\rm TF}$-axis.

The distributions of $\mu_{\rm TF}$ in the $\log {V_{\rm M}}^{\rm n}$ intervals are shown in Fig. 3. The bins on $\mu_{\rm TF}$ should have the width $5 \cdot 1.082 \cdot 0.2/k$, ($k$ =1,2,3,...) in order to collect the same $\log d_{25}$ ranges on the individual $\mu_{\rm TF}$ distributions as expected from the $\log V_{\rm M}$ intervals (0.2) and the slope of the diameter TF relation (1.082). Selecting $k = 2$, we get suitable bin size $\Delta\mu = 0.541$. For clarity, Fig. 4 shows the distributions artificially shifted on the $\mu_{\rm TF}$-axis, revealing their similar forms.

The next step is the normalization of the numbers $\log N$. For this we use the following procedure:

1. Select the complete part of the $\log d_{25}$ distribution. The putative limit is $\log d_{25} = 1.2$, as expected from previous studies.
2. Find the corresponding part of the first subsample (with smallest $\log {V_{\rm M}}^{\rm n}$) and count the total number of galaxies below and at $\mu_{\rm lim}(1) = 30.5$: $N(1, \mu_{\rm lim}(1))$.
3. For the second subsample calculate $N(2, \mu_{\rm lim}(1))$.
4. Shift curve 2 by $\Delta \log N = \log N(1, \mu_{\rm lim}(1)) - \log N(2, \mu_{\rm lim}(1))$.
5. Normalize the remaining curves using the same procedure with increasing $\mu_{\rm lim}$ by the shift between the subsequent curves. In this manner we utilize progressively deeper complete parts. Then the cumulative correction for the j:th curve is

$$\Delta_j \log N = \sum_{i=2}^{j} \left[\log N(i-1, \mu_{\rm lim}(i-1)) - \log N(i, \mu_{\rm lim}(i-1))\right],$$

where $\mu_{\rm lim}(i) = \mu_{\rm lim}(i-1) + 0.541$. By restricting the steps in this manner, we keep progressively farther from the putative limit $log d_{25} = 1.2$, while having an increasing number of galaxies available for normalization.

Figure 5 shows the resulting normalized composite distribution. One may note two particular things: There is first a rather scattered run of points up to about $\mu_{\rm TF} = 31$ which can be roughly approximated by a $0.6\mu_{\rm TF}$ line. After that the common envelope assumes a shallower slope of about 0.46.

Using now the points above $\log d_{25} = 1.2$ for each curve and requiring that each point contains more than 12 galaxies, by which the noisy $\mu_{\rm TF}$ ranges are removed, we draw a straight line through them. For this line, there are points up to $\mu_{\rm TF} = 34$. We use this line, derived by simple least-squares technique, as a reference for further study of the density law using information from the incomplete parts of the μ - distributions. This "envelope line" is shown in Fig. 6 together with points from the incomplete parts where we again use only those which contain more than 12 galaxies The average $\langle \log d_{25} \rangle$ is written besides each symbol. One can easily discern the sequences corresponding to the same positions in the $\log d_{25}$ distributions (c.f. points A and B in Fig. 1). These averages do not vary much along the same sequence. Comparing with the line of slope 0.46 inserted, one sees that the sequences follow rather well this slope, similarly as was found above for the points in the complete part (especially above $\mu_{\rm TF} \approx 31$).

We tested the completeness limit by assuming limits at $\log d_{25} = 1.3$ and 1.4 instead of the above $\log d_{25} = 1.2$. With these more conservative values we can be more certain of the completeness of the sample, however at the price of reduced number of data points. We got slopes 0.46 ($\pm$0.01) and 0.43 ($\pm$0.02) for limits 1.3 and 1.4 re-

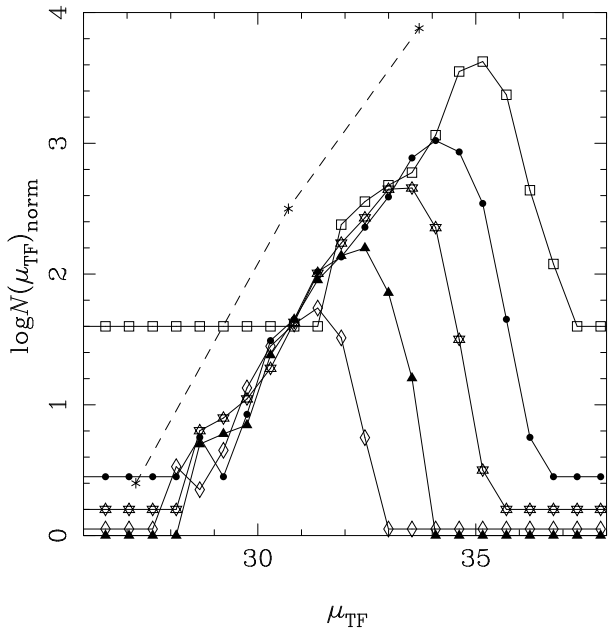

Fig. 5. Normalized composite distribution, constructed from the distributions of Fig. 3 by the steps described in the text. Note the appearance of a good envelope line. The inserted dotted lines have slopes 0.6 and 0.46. $\log N = 0$ levels are conveniently identified as horizontal parts.

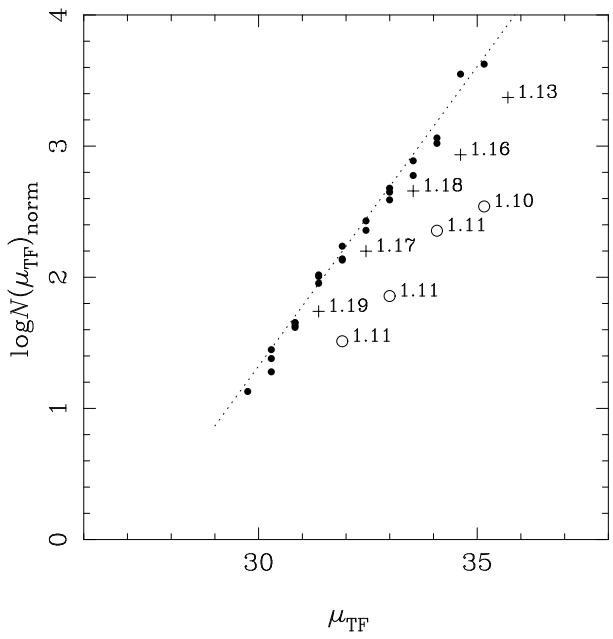

Fig. 6. The envelope line from Fig. 5 (shown as dotted line), together with points from the incomplete parts. The dots represent the envelope points and other symbols refer to incomplete parts. The numbers besides the latter give $\langle \log d_{25} \rangle$ and allow one to easily recognize the sequences following a slope close to 0.46 (envelope line).

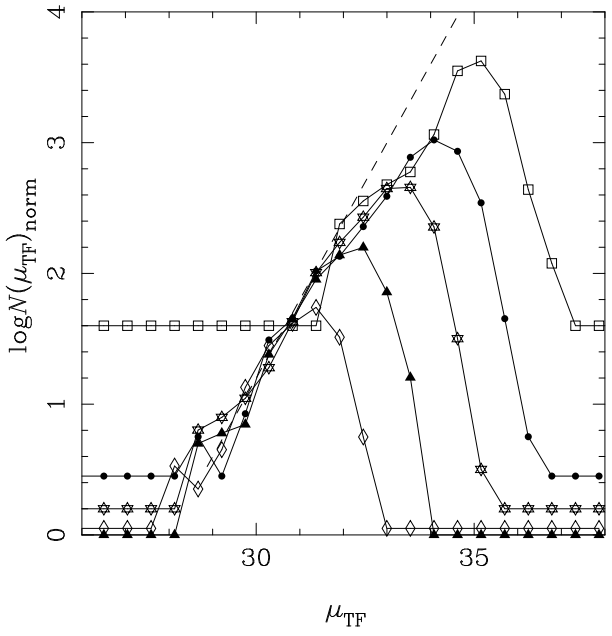

Fig. 7. The line of slope 0.6 forced to go through the first normalization point. In this case the incompleteness is seen to increase together with $\log V_{\rm M}$.

spectively, but the "envelope lines" in both cases were not as well defined as before. For now, we are more satisfied with the completeness limit at $\log d_{25} = 1.2$ giving us the slope 0.46 (see also Sect. 3.4 for another test, using simulated galaxy samples).

Naturally, all this is interestingly close to 0.44 predicted on the basis of fractal dimension $\mathcal{D} \approx 2.2$, as obtained e.g in the Di Nella et al. (1996) correlation analysis of LEDA. However, we are well aware that systematic effects may be involved, when we are working rather close to the completeness limit of the KLUN-sample. We have attempted to find any systematic error that could explain the shallower than 0.6 slope and have also looked what happens when one forces a line of slope 0.6 to start at $\mu_{\rm TF} = 31$. In Fig. 7 this has been done, and the line which rather well describes the (scattered) run of data below $\mu_{\rm TF} = 31$, systematically deviates from the envelopes of the normalized distributions at larger $\mu_{\rm TF}$. This behaviour implies that if the deviation from the 0.6μ-law is due to incompleteness problem, the incompleteness in apparent size starts for different $\log V_{\rm M}$ ranges at different $\log d_{25}$. This is something that we cannot understand, because the needed effect is quite large. For the largest $\log V_{\rm M}$ it means that incompleteness starts around $\log d_{25} = 1.7$, while for the smallest $\log V_{\rm M}$ such a limit would be around 1.2 (in terms of magnitudes this corresponds to a difference of about 2.5 mag). Still another way to state the problem is that if we try to shift the maxima of the distributions to follow the 0.6μ-slope, the curves are everywhere separated, there is no normalization and no common envelope. A

clear argument against such a large effect comes also from the method of normalized distances used in Theureau et al. (1997b): in the "unbiased plateau" produced as a part of the method, one should readily recognize such differences in the selection functions of galaxies with small and large $\log V_{\rm M}$. Also, from the manner of how KLUN was created as a diameter limited sample, independent of any considerations of $\log V_{\rm M}$, there is no reason to expect so significant dependence of the selection on $\log V_{\rm M}$. For instance, a recent analysis of the H I line profile detection rates at Nançay radio telescope by Theureau et al. (1997c) does not give any indication that large $\log V_{\rm M}$ galaxies are significantly underrepresented in KLUN.

Finally, if erroneous, the present slope 0.46 is just by an accident very close to ones obtained by several quite different correlation analyses (e.g. Sylos Labini et al. 1998a).

3.2. Magnitude TF distance moduli

The B-magnitude TF relation has smaller scatter than the diameter relation, which makes it tempting to use also it in this study even though the numbers are then smaller and the selection properties of the resulting sample are complicated by the fact that KLUN has been originally selected on the basis of apparent size. However, if the distribution of the galaxies of different $\log V_{\rm M}$ ranges is the same in the $\log d_{25}$ – B_T plane, one can use the magnitude relation in a similar manner.

We do not go through the steps in such detail as for the diameter distance moduli. Figure 8 shows directly the normalized composite diagram. Because of the underlying diameter limit, the incompleteness begins farther from the maxima than in the case of diameters, and the complete part of the envelope is now shorter in $\mu_{\rm TF}$. The envelope line constructed from points below the putative magnitude limit $B = 13.25$, is also shown. It has now the slope 0.40. Because the numbers of galaxies at each point of this diagram are smaller than in Fig. 5, the error of the slope is slightly larger than when using diameters ($\sigma = 0.012$, compared to $\sigma = 0.010$ with diameters). Inspection of the points in the incomplete part shows that the sequences, analogous to what was discussed for the diameter moduli, have similar slopes. However, now the achievable μ-ranges and numbers are smaller, and we do not show them separately.

3.3. Systematic error caused by finite $\log V_{\rm M}$ *ranges*

One can see a systematic effect in this method where we are forced to use finite $\log V_{\rm M}$ ranges instead of ideal infinitesimals. It comes from the fact that galaxies are not quite similarly distributed inside the different $\log V_{\rm M}$ ranges. The distribution of $\log V_{\rm M}$ has a maximum. Because of the form of the $\log V_{\rm M}$ distribution, inside the small - $\log V_{\rm M}$ interval one expects an increasing number density of galaxies towards the edge with larger $\log V_{\rm M}$,

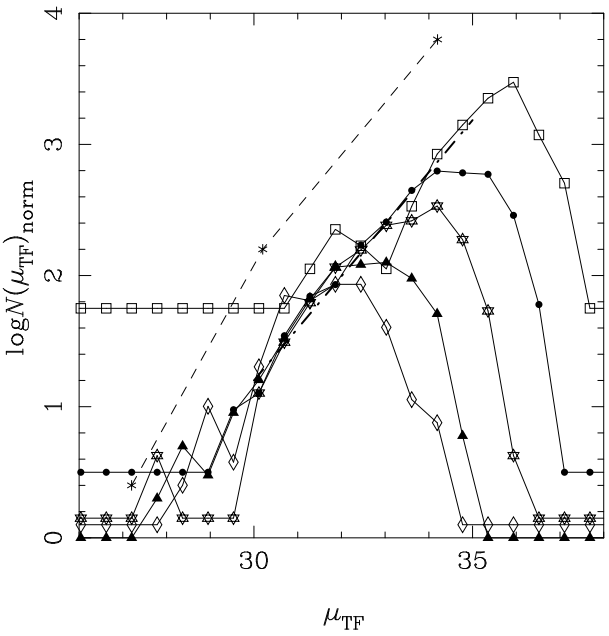

Fig. 8. Normalized composite distribution for B-magnitude TF distance moduli in different $\log {V_{\rm M}}^{\rm n}$ ranges. The slopes 0.6 and 0.4 are shown as well as the envelope line.

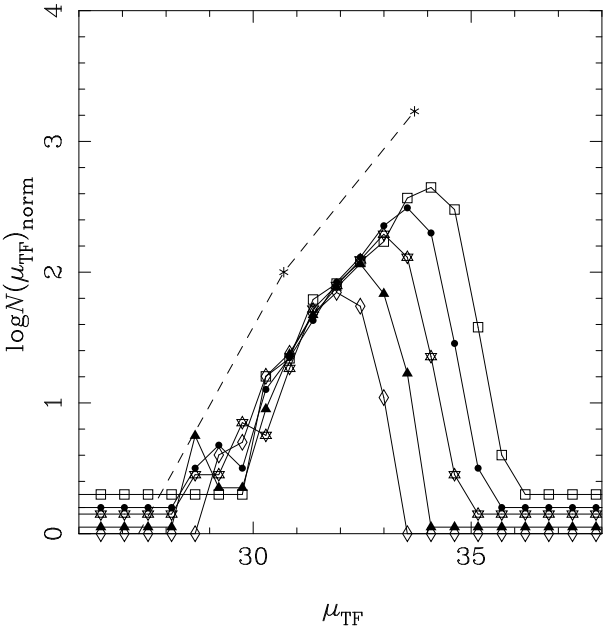

Fig. 9. Normalized composite distribution for diameter TF distance moduli, constructed as Fig. 5, but using intervals of 0.1 in $\log {V_{\rm M}}^{\rm n}$ in the range 1.7 – 2.3. Note the appearance of a good envelope line. The inserted dotted lines have slopes 0.6 and 0.41.

while for the large - $\log V_{\rm M}$ range this trend is reversed (see Fig. 2). In Fig. 6 one sees that the averages $\langle \log d_{25} \rangle$ within different sequences do not vary very much which suggests that the effect is actually not very important.

In order to check whether decreasing the interval size influences the result obtained above, we made an experiment whereby $\log {V_{\rm M}}^{\rm n}$ interval was reduced to 0.1, in the range 1.7 – 2.3, where the numbers of galaxies remain large enough. Now the slope of the envelope line is 0.41, the furthest point of the line being slightly above 100 Mpc (Fig. 9). Again, the diminished number of galaxies make error of the slope larger, $\sigma = 0.015$, while $\sigma = 0.010$ in Fig. 5.

3.4. Numerical experiment using simulated galaxy sample

In order to check further the reliability of the used method, we have made numerical experiments with simulated galaxy samples. In making these tests, we have kept in mind the following points:

1. Because individual distance moduli have considerable scatter and because we are interested in the all-sky averaged behaviour of radial density, the present method and the available data allow one to derive a quite smoothed-out view of the space density around the Galaxy.
2. The all-sky average, as derived by the present method, does not make a difference between a random distribution of galaxies with a radial density variation and a fractal distribution with the corresponding fractal dimension. Hence, for the purpose of testing systematic errors in the method, it is sufficient to consider simulated distributions, where randomly scattered galaxies have a smooth radial density variation.
3. The all-sky averaged radial distribution inside a fractal structure is statistically the same around all galaxies, which gives special motive for applying the present method. In non-fractal structures, such as supercluster-void network (e.g. J. Einasto et al. 1997), the radial distribution depends on the position of the observer (though in many cases the presence of the plane gives an apparent $\mathcal{D} \approx 2$, also reflected in correlation function analysis where actually an average of all the observers is taken, see the models by Einasto 1992). It is intended to extend the present method to study large individual structures in specified regions of the sky detected previously with redshift-distances (such as the Great Wall). Such applications will need specially tailored simulations which show how the method draws the density distribution curve, say, through a narrow plane of galaxies.

In the experiments we started with large number of galaxies (say 10^5), for which we alloted radial distances using an input value of the radial density gradient $\alpha = \alpha_{\rm in}$ in the density law $\log N = \alpha\mu +$ const. For each galaxy we chose a random absolute diameter from a gaussian distribution with $\log D_{\rm abs,0} = 1.3$ and $\sigma = 0.18$ ($D_{\rm abs}$ in kiloparsecs). Even though the $\log D_{\rm abs}$ distribution in reality hardly is gaussian, it is not too far from the truth for the KLUN sample. All the galaxies having apparent diameter larger than limit $\log d_{\rm lim}$ were included in the "observed subsample". To make this observed sample more realistic we also allowed in some galaxies below the diameter limit, percentage of included galaxies being progressively smaller further below the $d_{\rm lim}$. Each of these observed galaxies were then given a rotational parameter $\log V_{\rm M}$ by inverse TF relation ($\log V_{\rm M} = a' \log D_{\rm abs} + b'$) with $a' = 0.5$, $b' = 1.13$ and a gaussian dispersion $\sigma = 0.15$. These values resemble results of the recent KLUN study (Theureau et al. 1997a). Now the $\log N - \mu_{\rm TF}$ graph (distance moduli from *direct* TF relation) for the observed subsample could be investigated as above was done for the real KLUN sample.

First we selected $\log d_{\rm lim} = 1.2$ and varied the density gradient $\alpha_{\rm in}$. For each $\alpha_{\rm in}$ we chose the initial number of galaxies so that the number of observed galaxies was the same as in KLUN sample. Then we calculated the slope of the "envelope" line in the $\log N - \mu_{\rm TF}$ graph getting the observed density gradient $\alpha_{\rm obs}$ For each $\alpha_{\rm in}$ we repeated the simulation 1000 times to get $\langle \alpha_{\rm obs} \rangle$ with error bars. For every $\alpha_{\rm in}$ the resulting $\langle \alpha_{\rm obs} \rangle$ was smaller than $\alpha_{\rm in}$. However, this tendency was not large enough to explain

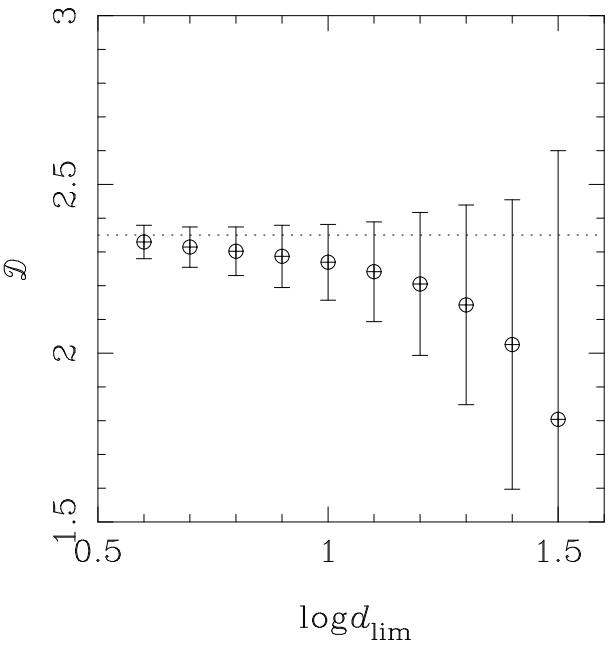

Fig. 10. Test of the apparent diameter completeness limit $\log d_{\rm lim}$ using simulated galaxy samples. Dotted line shows the input value of density gradient $\alpha = 0.47$, which corresponds to fractal dimension $\mathcal{D} = 2.35$. For more complete samples (smaller $\log d_{\rm lim}$) the observed $\mathcal{D}$ approaches the input value. Error bars are mean deviations (2σ) for 1000 simulations. $\log d_{\rm lim} = 1.2$ is the completeness limit assumed for KLUN.

the deviation of our observed slope (in this section we use as a reference point $\alpha = 0.44$, which is a weighed average of the slopes obtained with diameters and magnitudes) from homogeneous galaxy distribution ($\alpha = 0.6$). The simulations showed that for $\alpha_{\rm obs} = 0.44$, $\alpha_{\rm in} = 0.47 \pm 0.04$ (2σ errors). In terms of fractal dimension ($\alpha = 0.2\mathcal{D}$) we can say that the observed value $\mathcal{D} = 2.2$ can be affected by our methods so that the true value is $\mathcal{D} \approx 2.35 \pm 0.20$.

We then tested the effect of the completeness limit by varying $\log d_{\rm lim}$, while keeping the other parameters fixed. Figure 10 shows how $\mathcal{D}_{\rm obs} \rightarrow \mathcal{D}_{\rm in}$ when the sample gets more complete. Also, with smaller completeness limits the number of observed points increase, and the errors get smaller. This emphasizes the importance of expanding the database to make it deeper and more complete.

4. Discussion and concluding remarks

As it appears from the preceding analysis, we have arrived at the conclusion that KLUN galaxies seem to indicate a "thinning" of the galaxy universe from $\mu_{\rm TF} \approx 31$ up to ≈ 36. In order to see the actual range, the distance moduli must be corrected for the Malmquist bias of the first kind which in the case of $\mathcal{D} = 2$ becomes $\mathcal{D}/3\times\ 1.382\ \sigma_M^2 = 0.92\sigma_M^2$ for the magnitudes and $\mathcal{D}/3\times\ 5 \times 5 \times 1.382\sigma^2_{\log D} = 23.05\sigma^2_{\log D}$ for the diameters (see e.g. Teerikorpi 1997). Using $\sigma = 0.5$ mag and $= 0.15$ for magnitudes and (log)diameters, respectively, these corrections make the maximal distance probed by both the diameter and magnitude relations about 200 Mpc, corresponding to the first point beyond the maximum of the highest $\log V_{\rm M}$ distribution.

This result, using photometric distances independently of redshifts, and an all-sky sample, offers a complementary piece of evidence for the debate on the dimension and maximum scale of fractality. The value $\mathcal{D} \approx 2$ which has appeared in several correlation studies (Klypin et al. 1989, Einasto 1991, 1992, Guzzo et al. 1991, Calzetti et al. 1992, Di Nella et al. 1996, Guzzo 1997, Sylos Labini et al. 1998a), is here seen as a density law up to 200 Mpc, the limit of the KLUN sample. Taken alone, the present study does not prove any large scale fractality, it only suggests the existence of such an average density law around us (which in a restricted distance range could be caused by filamentary structure and voids or a large flattened system; Einasto 1992, Einasto et al. 1994, Paturel et al. 1994). On the other hand, within the framework of a large scale fractal distribution, our position on a peak surrounded by a decreasing density is as expected (Mandelbrot 1982). In this sense, when considered together with large scale correlation studies leading to $\mathcal{D} \approx 2$, the present result is consistent with the view that the Milky Way occupies a typical position in the fractal structure. This agrees with recent studies by Karachentsev (1996) and Governato et al. (1997) who conclude that the Local Group is a typical representation of other small groups, both in structure and environmental dynamics.

The result of our work is also consistent with recent results on the supercluster–void network (M. Einasto et al. 1994, 1997) and arguments based on the correlation analysis of rich clusters of galaxies (Einasto & Gramann 1993, J. Einasto et al. 1997). These studies claim that the observed transition scale to homogeneity is about 200–300 Mpc.

In view of local structures, fractal or not, we would not expect any perfect 0.6μ-law. Nevertheless, we have tried to understand if such a strong deviation from a homogeneous distribution could be due to some systematic error. However, numerical tests have shown that the method works, though it tends to somewhat underestimate the density gradient.

Naturally, the present study must be seen as a first step which uses distance moduli in the described manner and the method must be developed along with the increasing size of KLUN. A promising prospect is offered by the ongoing DENIS project (collecting 200000 galaxies by 1999) and the FORT project improving the efficiency of the Nançay radio telescope (see Theureau 1997). A deeper sample will allow us to better recognize systematic errors and the real space density trend.

Acknowledgements. We are grateful to Prof. Jaan Einasto for his very useful critisism. M.H. thanks for support by Finnish Culture Foundation, M. Ehrnrooth's Endowment and A. Kordelin's Cultural and Educational Foundation. Yu.B. thanks for support by the Russian program "Integration" project N. 578. This work has been supported by Academy of Finland (project "Cosmology in the Local Universe"). We have used data from the Lyon-Meudon Extragalactic Database (LEDA) compiled by the LEDA team at the CRAL – Observatoire de Lyon (France).

References

Baryshev, Yu. 1981, Izvestija SAO, 14 24
Calzetti, D., Giavalisco, M., Meiksin, A. 1992, ApJ 398, 429
Davis, M. 1997, in the Proceedings of the Princeton Conference "Critical Dialogues in Cosmology", ed. N. Turok (World Scientific)
Di Nella , H., Montuori, M., Paturel, G., Pietronero, L., Sylos Labini, F. 1996, A&A 308, L33
Einasto, J., Gramann, M. 1993, ApJ 407, 443
Einasto, J., Einasto, M., Frisch, P. et al. 1997, MNRAS 289, 801
Einasto, M. 1991, MNRAS 252, 261
Einasto, M. 1992, MNRAS 258, 571
Einasto, M., Einasto, J., Tago, E., Dalton, G., Andernach, H. 1994, MNRAS 269, 301
Einasto, M., Tago, E., Jaaniste, J., Einasto, J., Andernach, H. 1997 A&AS 123, 119
Governato, F., Moore, B., Cen, R., Stadel, J., Lake, G., Quinn, T. 1997, New Astronomy 2, 91
Guzzo, L. 1997, New Astronomy 2, 517

Guzzo, L., Iovino, A., Chincarini, G., Giovanelli, R., Haynes, M. 1991, ApJ 382, L5
Karachentsev, I. 1996, A&A 305, 33
Klypin, A., Einasto, J., Einasto, M., Saar, E. 1989, MNRAS 237, 929
Mandelbrot, B. 1982, The Fractal Geometry of Nature (Freeman, New York)
Paturel, G., Bottinelli, L., Di Nella, H. et al. 1994, A&A 289, 711
Peebles, P.J.E. 1980, The Large Scale Structure of the Universe (Princeton University Press)
Pietronero, L., Montuori, M., Sylos Labini, F. 1997, in the Proceedings of the Princeton Conference "Critical Dialogues in Cosmology", ed. N. Turok (World Scientific)
Praton, E., Melott, A., McKee, M. 1997, ApJ 479, L15
Sylos Labini, F., Gabrielli, A., Montuori, M., Pietronero, L. 1996, Physica A 226, 195
Sylos Labini, F., Montuori, M., Pietronero, L. 1998a, Physics Reports (in press)
Sylos Labini, F., Montuori, M., Pietronero, L. 1998b, New Astronomy (submitted, preprint: astro-ph/9801151)
Teerikorpi, P. 1993, A&A 280, 443
Teerikorpi, P. 1997, Ann. Rev. A&A 35, 101
Theureau, G. 1997, Thèse de Doctorat (Paris Observatory)
Theureau, G., Hanski, M., Teerikorpi, P. et al. 1997a, A&A 319, 435
Theureau, G., Hanski, M., Ekholm, T. et al. 1997b, A&A 322, 730
Theureau, G., Bottinelli, L., Coudreau, N. et al. 1997c, A&AS (in press)
Witasse, O., Paturel, G. 1997, A&A 321, 10

This article was processed by the author using Springer-Verlag LaTeX A&A style file *L-AA* version 3.